International Orthopaedics (2023) 47:241–249
https://doi.org/10.1007/s00264-022-05622-8

ORIGINAL PAPER

Fracture mapping of intra-articular calcaneal fractures

Boyu Zhang[1,2] · Hao Lu[1,2] · Yuan Quan[1,2] · Yi Wang[3] · Hailin Xu[1,2]

Received: 22 August 2022 / Accepted: 22 October 2022 / Published online: 4 November 2022

Abstract

Background Calcaneal fractures have complex morphology, which brings great challenges to clinical treatment. The primary fracture lines could help us simplify the fracture. Fracture mapping technology can help surgeons understand the fracture morphology more intuitively. This study aims to develop a further understanding of calcaneal fractures by delineating the primary fracture lines through the fracture mapping technology.

Methods Ninety cases of intra-articular calcaneal fractures were reviewed between March 2016 and January 2019 at a level 1 trauma centre. The CT data of these cases were reconstructed and reduced using software. We superimposed the primary fracture lines on a standard model and created the distribution and heat map of the intra-articular calcaneal fractures. SPSS 18.0 was used to count the differences between the different groups.

Results The primary fracture lines concentrated at the Gissane angle and the posterior articular surface, which could be summarized in two ring structures. There were 43 cases of fracture involving calcaneocuboid joint, including 32 cases of joint-depression fracture and 11 cases of tongue-type fracture. The area ratio of lateral fragment of simple tongue-type fracture is larger than joint-depression fracture.

Conclusion The primary fracture lines of calcaneus were distributed in two rings on the surface of calcaneus. Based on the distribution of primary fracture rings, we integrated the classification of calcaneal fracture and proposed some treatment recommendations.

Keywords Calcaneal fracture · Fracture mapping · Morphology · Fracture ring

Introduction

Calcaneal fractures are the most common tarsal fractures, accounting for about 2% of total body fractures. Approximately 60 to 75% of calcaneal fractures are intra-articular fractures [1–3]. Calcaneal fractures often occur in young physical laborers, and many patients have different degrees of physical activity disorders in the long term [4, 5]. At present, the treatment of calcaneal fractures is still controversial. Displaced intra-articular fractures are surgical indications for calcaneal fractures. One of the main objectives of surgery is to restore the posterior articular surface and reduce the occurrence of long-term subtalar arthritis. Timely and accurate identification of calcaneal fractures is essential for subsequent surgical plans.

There are a variety of classification systems for calcaneal fractures, each with a different emphasis. At present, the most common clinical classifications are Essex-Lopresti classification and Sanders classification. Essex-Lopresti divides intra-articular calcaneal fractures into two categories, tongue type fracture and joint-depression fracture, which described the morphology of the fracture fragment and could provide guidance for treatment of calcaneal fractures [6]. Sanders classified calcaneal fractures by the number and location of fracture fragments on the posterior articular surface of calcaneus on coronal and axial CT images, which could make predictions about patients' outcomes [7]. Despite this classification has been widely used in the clinic, it still has limitations on concordance and inability to guide the surgical procedures [8–10].

Boyu Zhang, and Hao Lu, equally contributed to this work.

✉ Hailin Xu
xuhailinfa@163.com

[1] Orthopaedic and Traumatology, Peking University People's Hospital, No. 11 Xizhimen South Street, Beijing 100044, China

[2] Key Laboratory of Trauma and Neural Regeneration (Peking University), Ministry of Education, Beijing, China

[3] Department of Anesthesiology, Peking University People's Hospital, Beijing, China

In 1989, Carr et al., based on morphological study of cadaver bones, proposed that there were two primary fracture lines in sagittal and coronal positions for calcaneal fractures, which divided the calcaneus into different major fracture fragments [11]. Since the main fracture line involves the articular surface of the calcaneus, the morphology of the major fracture fragments determines the treatment and outcome of the patients.

Fracture mapping was first applied to scapular fractures in 2009 by Armitage et al. [12]. Fracture mapping technology, through three-dimensional reconstruction of CT data, superimposes fracture lines of multiple cases on the same standard template to obtain the distribution of the fracture lines, which further helps clinicians better understand the mechanism and morphology of fractures, and formulate treatment procedures. Currently, fracture mapping technology has been used in the proximal humerus, distal radius, ankle, spine, and other fractures of the whole body [13–17]. The aim of this study was to map primary fracture lines and incorporate these in to a combined classification system with specific treatment recommendations.

Materials and methods

Eligibility criteria

Patients with calcaneal fractures between March 2016 and January 2019 were reviewed. The inclusion criteria were as follows: (1) age ≥ 18 years; (2) intra-articular calcaneal fracture; (3) CT scanning layer thickness ≤ 3 mm. The exclusion criteria were as follows: (1) previous history of foot trauma or surgery on the affected side; (2) pathological fracture; (3) old calcaneal fracture; (4) difficulty in reconstructing the fragments.

Fracture mapping

CT images of all patients in digital imaging and communications in medicine (DICOM) format were imported into mimics 20.0 software (materials, Leuven, Belgium), and the fracture fragments were reconstructed, segmented, and reduced. All data were exported into 3-Matic 12.0 software (materials, Leuven, Belgium). The mirror, translation, and rotation functions were used to match the reduced calcaneal fracture model with the standard 3D calcaneal model (reconstructed by a healthy volunteer), and the line of fracture was delineated on the standard model. Finally, the primary fracture lines were imported into e-3D software (Central South University, Changsha, China) to create heat map of the fracture lines.

Data analysis

We characterized the fracture line heat maps from four directions: anterior, superior, medial, and lateral, with different color areas indicating different frequency of fracture line involvement within the region (gradually rising from blue to red). SPSS 18.0 software (IBM, Armonk, NY) was used for Chi-square analysis of patients with different Essex-Lopresti classification. Mann–Whitney test was used to analyze the proportion of fracture fragment area on articular surface of different fracture groups. A value of $P < 0.05$ was considered as significant difference.

Results

Patient characteristics

A total of 90 patients with CT data were included in this study. Sixty-nine patients were male and 21 were female. There were 42 cases of right foot and 48 cases of left foot. According to Essex-Lopresti classification, there were 35 tongue-type fractures and 55 joint-depression fractures. According to Sanders classification, there were 66 cases of Sanders type II, 19 cases of Sanders type III, and 5 cases of Sanders type IV. Patient characteristics are summarized in Table 1.

Fracture mapping

We grouped 90 cases of calcaneal fractures according to the number and shape of posterior articular fracture fragments: (1) simple tongue-type fractures (26 cases, 28.9%); (2) simple joint-depression fracture (40 cases, 44.4%); (3) comminuted fracture (24 cases, 26.7%) (posterior articular

Table 1 Characteristics of patients

Sex, *n* (%)	
Male	69 (76.7)
Female	21 (23.3)
Affected side, *n* (%)	
Left	48 (53.3)
Right	42 (46.7)
Sanders classification, *n* (%)	
Type II	66 (73.3)
Type III	19 (21.1)
Type IV	5 (5.6)
Essex-Lopresti classification, *n* (%)	
Joint-depression fracture	55 (61.1)
Tongue-type fracture	35 (38.9)

fragments equal 2 refers to simple fracture, and fragments more than 3 refers to comminuted fracture). According to the above grouping, we made the distribution map of primary fracture lines and heat map, respectively (Figs. 1, 2, and 3).

The primary fracture lines of calcaneal fractures are concentrated at the Gissane angle and extend posteriorly across the posterior articular surface to the calcaneal tuberosity, the fracture lines of the lateral wall extend from the Gissane angle, and the fracture lines of the medial wall run anteriorly and plantar around the sustentaculum tali process posteriorly in the tuberosity.

The fracture lines of a simple joint-depression fracture on the lateral wall are more sparse than those of the tongue-type fracture and the fracture lines of the medial wall are closer to the anterior. Compared to the simple fractures, comminuted fractures have a concentrated area of fracture lines on the lateral side of the anterior process extending forward to the calcaneocuboid joint.

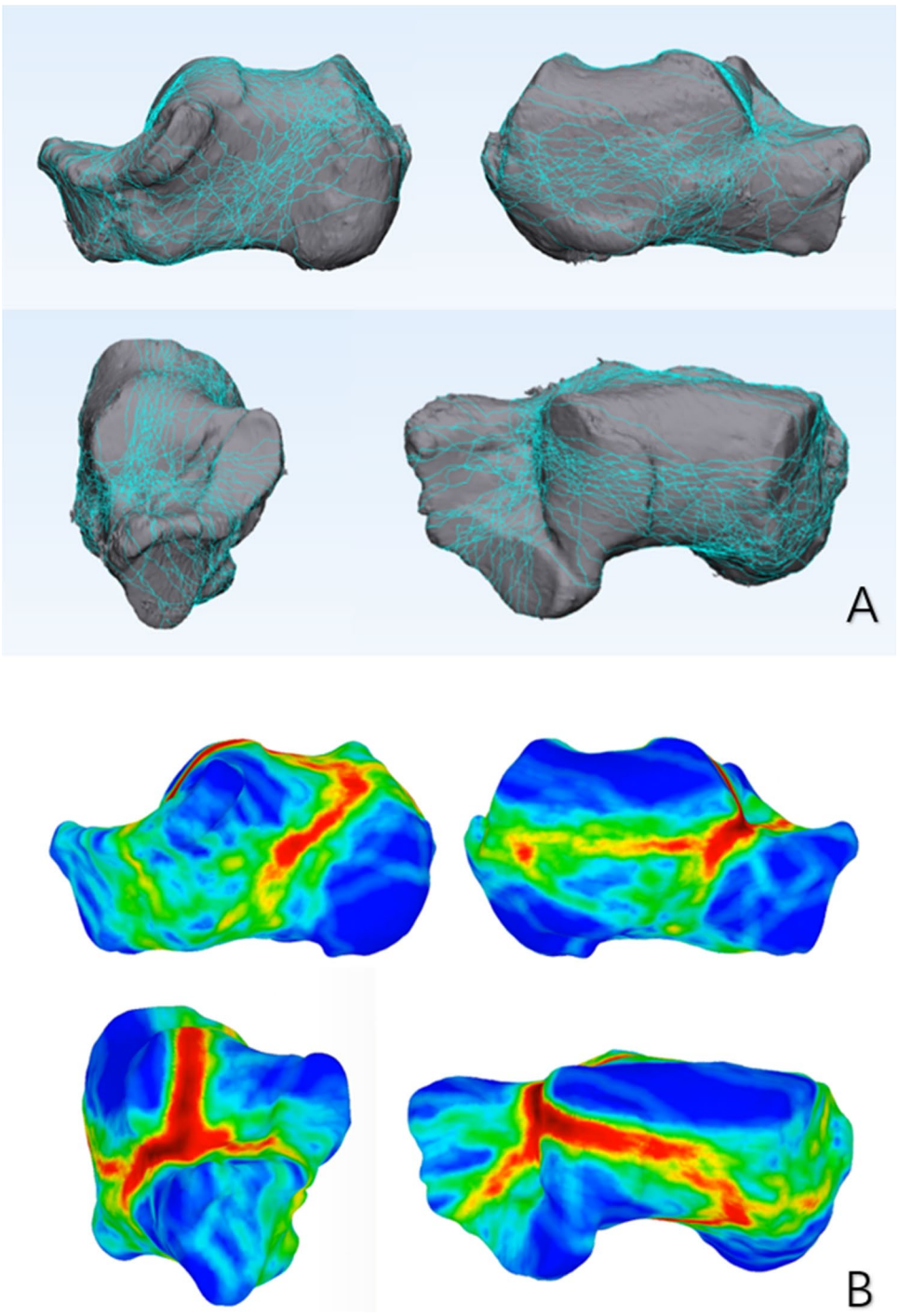

Fig. 1 Primary fracture lines of simple tongue type fractures on medial, lateral, anterior, and superior views. **A** Distribution map, **B** Heat map

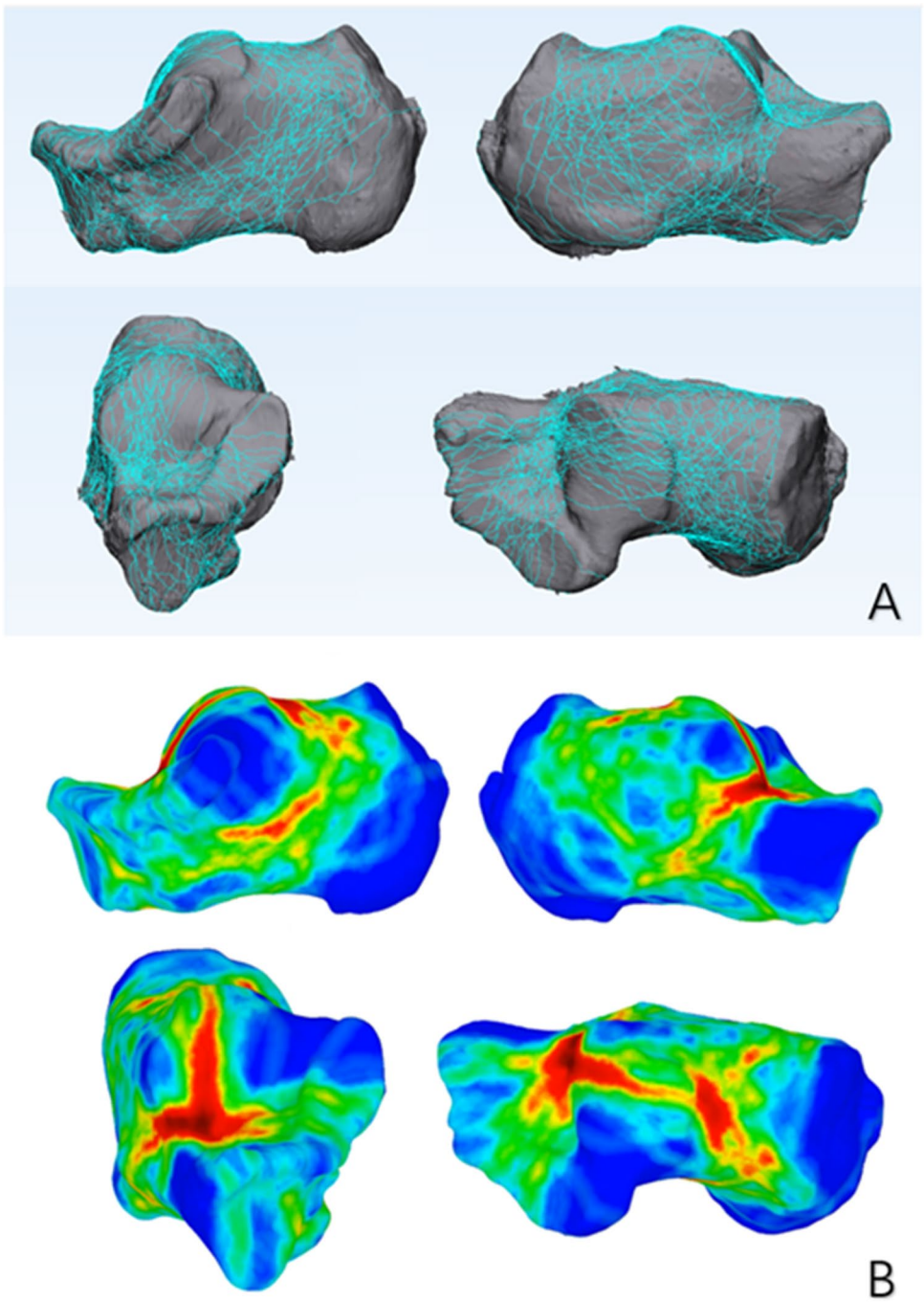

Fig. 2 Primary fracture lines of simple joint-depression fractures on medial, lateral, anterior, and superior views. **A** Distribution map, **B** Heat map

Calcaneocuboid joint involvement

Different types of calcaneal fractures have different rates of calcaneocuboid joint involvement. There were 43 cases of fracture involving calcaneocuboid joint, including 32 cases (74.4%) of joint-depression fracture and 11 cases (25.6%) of tongue-type fracture. Chi-square test showed statistical differences between them ($P < 0$ 0.05), as shown in Table 2.

Posterior articular surface fragment size

The distribution trend of primary fracture lines of simple tongue type fracture is similar to that of simple joint-depression fracture. On the posterior articular surface, the fracture

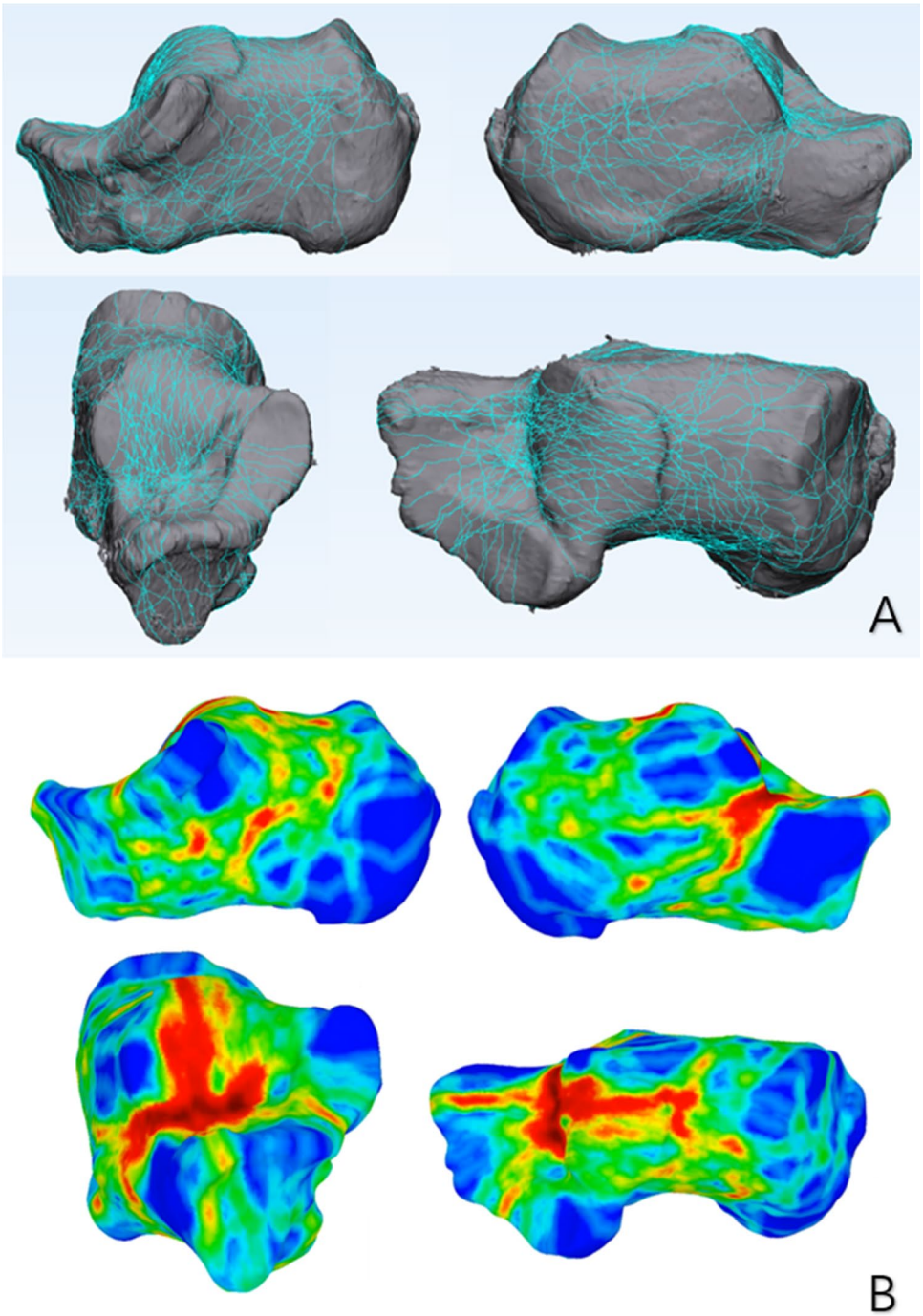

Fig. 3 Primary fracture lines of comminuted fractures on medial, lateral, anterior, and superior views. **A** Distribution map, **B** Heat map

Table 2 Calcaneocuboid joint involvement

	Involved	Uninvolved	χ^2	*P*
Tongue-type fracture	11	23	4.179	.041
Joint-depression fracture	32	24		

line of the tongue-type fracture is more medial than that of the joint-depression fracture. We measured the ratio of the area of the lateral fracture fragment to the area of the posterior articular surface. Mann–Whitney test showed that there was a statistical difference between the two groups ($P < 0\ 0.05$), as shown in Table 3.

Discussion

Calcaneal fractures are more common in high-energy injuries with complex fracture morphology, which is not conducive to the study of mechanism and treatment [4].

Table 3 Area ratio of lateral fragment of simple fracture

	Number	Median	Mean	SD	Sum of rank	*Z*	*P*
Tongue-type fracture	26	43.17%	46.62%	0.2083	1059	−2.467	.014
Joint-depression fracture	40	34.71%	34.37%	0.1772	1152		
Total	66	38.89%	39.19%	0.1980			

SD standard deviation

In 2021, Ni et al. first described the fracture line distribution of calcaneal fractures by fracture mapping technology. Through the analysis of 62 cases of complex intra-articular calcaneal fracture lines, it was found that the calcaneal fractures mainly involved the anterior border of the posterior articular surface, and the fractures rarely involved the sustentaculum tali, posterior calcaneal tuberosity, and anterior process [18]. In the same year, Guo et al. analyzed Sanders II joint-depression fracture and tongue-type fracture respectively through fracture mapping technology. In addition to describing the overall calcaneal fracture lines, they described in detail the fracture lines of calcaneal anterior process, and proposed different fixation recommendations for different subtypes of fractures [19, 20]. In 2022, Yu et al. reconstructed 226 intra-articular calcaneal fractures and drew a two-dimensional fracture map from six sections. This study was the first to associate the distribution of calcaneal fracture lines with the internal structure of the calcaneus, suggesting that the anatomical morphology of the talus and calcaneus and the internal structure of the calcaneus play a crucial role in calcaneus fracture [21].

The lateral and medial wall and plantar side of the calcaneus are often comminuted with multiple irregular fracture fragments. The previous fracture mapping studies of calcaneal fractures superimposed all the fracture lines on the standard template, and finally obtained the fracture line distribution map and heat map [18–21]. However, the treatment core of calcaneal fracture is the reduction of articular surface, and anatomical reduction is not required for the comminuted fragments on the side wall and plantar side. It is of little significance to represent these parts of fracture line in the heat map for the selection of clinical treatment methods and understanding of injury mechanism. Therefore, it is very important to simplify calcaneal fractures.

The primary fracture lines mentioned by Carr in 1989 divided the calcaneus into different major fracture fragments [11]. Through the study of the primary fracture line, we could Integrate the existing classification and proposed treatment recommendations. Sanders classification proposed in 1993 is actually the classification of calcaneal fractures through the position of the primary fracture line in the sagittal position [7]. In our study, we hid the secondary fracture lines of the medial walls, lateral walls, and the plantar side of the calcaneus, and created the distribution map and heat map of the primary fracture lines, which can help us better understand the morphology and treatment of calcaneal fractures.

Through the description of fracture lines of 90 patients with calcaneal fracture, we found that the primary fracture lines of calcaneus were distributed in two rings on the surface of calcaneus, and the calcaneus was divided into two main fracture fragments by two fracture rings. The lateral fracture ring originates from the Gissane angle, extends posteriorly to the calcaneal tuberosity through the posterior articular surface, then turns laterally to the lateral wall and finally returns to the Gissane angle. This fracture ring forms lateral calcaneal fracture fragment on the calcaneus. The medial fracture ring partially overlaps with the lateral fracture ring at the posterior articular surface and calcaneal tuberosity. It turns around the sustentaculum tali to the medial wall in the middle and rear of the calcaneal tuberosity, and then returns to the anterior process from the front of the middle joint to finally form the medial fracture ring, and divides the medial fracture fragment, which is attached to the triangular ligament complex and is in a relatively stable position in the calcaneal fracture (Fig. 4). Several of the fractures present an anterolateral fracture ring, which originates from Gissane angle, travels anteriorly from the anterior process, and involves the calcaneocuboid joint, eventually turning below the calcaneus to the lateral wall and returning to the Gissane angle, forming an anterolateral fracture fragment involving the calcaneocuboid joint. In our opinion, the treatment of calcaneal fractures is to match the lateral fracture ring with the medial fracture ring.

In contrast to Carr et al.'s study, we used fracture mapping technology to depict the primary fracture lines of the calcaneus, obtaining a more three-dimensional view of the primary fracture lines and the morphology of the main fracture fragment. According to the morphology of the main fracture fragment, the displaced calcaneal intra articular fractures were summarized into three types: type I: simple tongue type fracture; type II: simple joint-depression fracture; type III: comminuted fracture. Interestingly, the heat maps of the primary fracture lines for these three types of fractures are remarkably similar, which suggests that different types of intra-articular calcaneal fractures may have similar injury mechanisms. At the same time, combined with Athavale's research on calcaneal trabecular bone, we speculated that the position of the foot and the magnitude of the force can cause

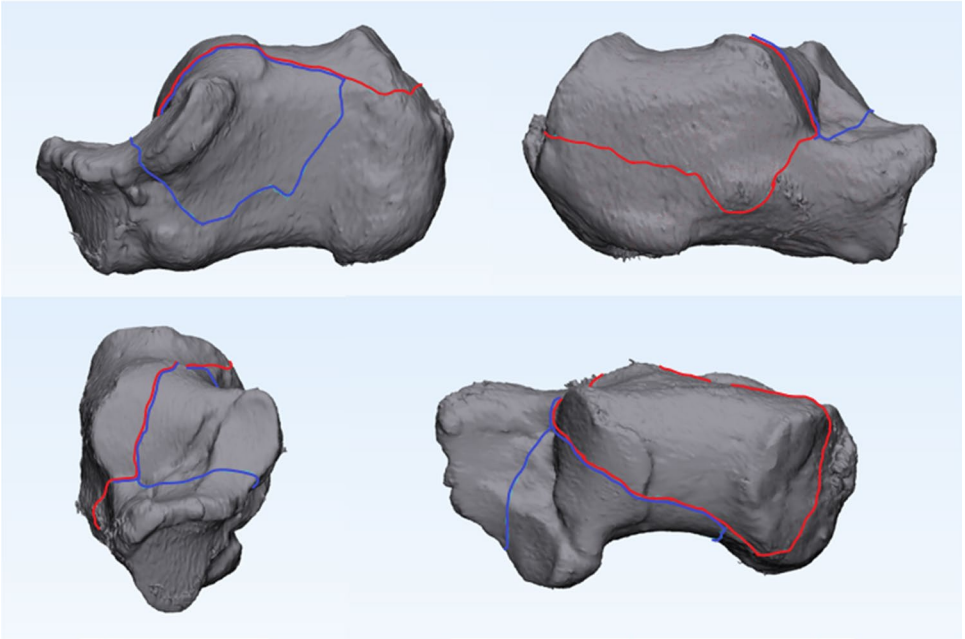

Fig. 4 The fracture rings (red: lateral ring; blue: medial ring)

the trabecular bone to break in different areas and produce different types of fracture [22].

Because joint-depression fractures are more common to involve the calcaneocuboid joint, we should evaluate type II fractures more carefully before operation and expand the incision to expose the calcaneocuboid joint if necessary. In the process of CT reconstruction and reduction of patients, we found that the shape of posterior articular surface fragments ≥ 3 (type III comminuted fracture) is not a simple 3-column or 4-column as described by Sanders et al. in the diagram [7]. We found that there were transverse fracture lines or small triangular bone blocks on the articular facet (Fig. 5), which could not be classified simply by Sanders classification. This type of fracture has different shapes of fracture fragments on the posterior articular surface and the heat map shows that the calcaneocuboid joint is involved in a high proportion, so more adequate exposure is needed during treatment [23].

Compared with previous fracture mapping studies of calcaneal fractures, we hide the secondary fracture lines on the surface of calcaneus for the first time, and depict the primary fracture lines of calcaneus and create the heat map [18–21]. Through the fracture map of the primary fracture lines of the calcaneus, we summarized the fracture lines on the calcaneus surface into two fracture rings for the first time, which could help us have a further understanding of the morphology and treatment of calcaneal fractures.

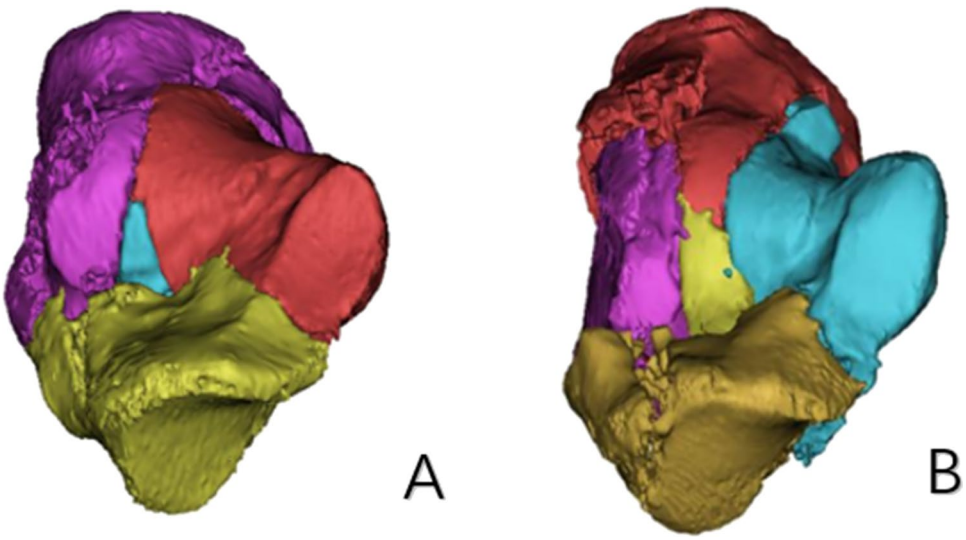

Fig. 5 Special fracture (**A** there is a triangular fracture fragment on the posterior articular surface; **B** there is a transverse fracture line on the posterior articular surface)

Our study has some limitations. Firstly, our study included a small number of cases and did not include non-displaced intra-articular calcaneal fractures, which may bias the results to some extent. Secondly, some complex fractures were excluded from this study due to the inability of effective reconstruction and reduction of some comminuted fractures. Finally, because the calcaneal morphology of each patient is not completely matched with the standard template, there will also be some bias in drawing the fracture line.

Conclusion

In this study, the morphology of calcaneus fractures was further understood by describing the main fracture lines of calcaneus. The main conclusions are as follows:

1. Despite differing levels of comminution and displacement, the primary fracture lines of the calcaneus, which could be summarized into two rings, are remarkably similar between classes of well-established clinical classification systems.
2. The calcaneocuboid joint is more common involved in joint-depression fractures.
3. The area of posterior articular surface involved in the lateral fracture fragment of tongue type fracture is larger.

Based on the distribution of primary fracture rings, we integrated calcaneal fractures and proposed some treatment recommendations.

Author contribution All authors contributed to the study conception and design. Material preparation, data collection and analysis were performed by Boyu Zhang, Hao Lu, Quan and Yi Wang. The first draft of the manuscript was written by Boyu Zhang and all authors commented on previous versions of the manuscript. All authors read and approved the final manuscript.

Declarations

Ethics approval This study was in accordance with the Declaration of Helsinki and approved by the Ethics Committee of Peking University People's Hospital (NO.2020PHB072-01).

Conflict of interest The authors declare no competing interests.

References

1. Marouby S, Cellier N, Mares O, Kouyoumdjian P, Coulomb R (2020) Percutaneous arthroscopic calcaneal osteosynthesis for displaced intra-articular calcaneal fractures: Systematic review and surgical technique. Foot Ankle Surg 26(5):503–8. https://doi.org/10.1016/j.fas.2019.07.002
2. Zhu Y, Li J, Liu S et al (2019) Socioeconomic factors and lifestyles influencing the incidence of calcaneal fractures, a national population-based survey in China. J Orthop Surg Res 14(1):423. https://doi.org/10.1186/s13018-019-1493-2
3. Zwipp H, Rammelt S, Barthel S (2004) Calcaneal fractures–open reduction and internal fixation (ORIF). Injury 35(2):Sb46-54. https://doi.org/10.1016/j.injury.2004.07.011
4. Mitchell MJ, McKinley JC, Robinson CM (2009) The epidemiology of calcaneal fractures. Foot (Edinb) 19(4):197–200. https://doi.org/10.1016/j.foot.2009.05.001
5. Humphrey JA, Woods A, Robinson AHN (2019) The epidemiology and trends in the surgical management of calcaneal fractures in England between 2000 and 2017. Bone Joint J. 101-b(2):140–6. https://doi.org/10.1302/0301-620x.101b2.Bjj-2018-0289.R3
6. Essex-Lopresti P (1952) The mechanism, reduction technique, and results in fractures of the os calcis. Br J Surg 39(157):395–419. https://doi.org/10.1002/bjs.18003915704
7. Sanders R, Fortin P, DiPasquale T, Walling A (1993) Operative treatment in 120 displaced intraarticular calcaneal fractures. Results using a prognostic computed tomography scan classification. Clin Orthop Relat Res 290:87–95
8. Jiménez-Almonte JH, King JD, Luo TD, Aneja A, Moghadamian E (2019) Classifications in brief: Sanders classification of intraarticular fractures of the calcaneus. Clin Orthop Relat Res 477(2):467–71. https://doi.org/10.1097/corr.0000000000000539
9. Howells NR, Hughes AW, Jackson M, Atkins RM, Livingstone JA (2014) Interobserver and intraobserver reliability assessment of calcaneal fracture classification systems. J Foot Ankle Surg 53(1):47–51. https://doi.org/10.1053/j.jfas.2013.06.004
10 Bhattacharya R, Vassan UT, Finn P, Port A (2005) Sanders classification of fractures of the os calcis. An analysis of inter- and intra-observer variability. J Bone Joint Surg Br 87(2):205–8. https://doi.org/10.1302/0301-620x.87b2.15260
11 Carr JB, Hamilton JJ, Bear LS (1989) Experimental intra-articular calcaneal fractures: anatomic basis for a new classification. Foot Ankle 10(2):81–7. https://doi.org/10.1177/107110078901000206
12. Armitage BM, Wijdicks CA, Tarkin IS et al (2009) Mapping of scapular fractures with three-dimensional computed tomography. J Bone Joint Surg Am 91(9):2222–8. https://doi.org/10.2106/jbjs.H.00881
13 Hasan AP, Phadnis J, Jaarsma RL, Bain GI (2017) Fracture line morphology of complex proximal humeral fractures. J Shoulder Elbow Surg 26(10):e300–e8. https://doi.org/10.1016/j.jse.2017.05.014
14. Misir A, Ozturk K, Kizkapan TB et al (2018) Fracture lines and comminution zones in OTA/AO type 23C3 distal radius fractures: The distal radius map. J Orthop Surg 26(1):2309499017754107. https://doi.org/10.1177/2309499017754107
15 Quan Y, Lu H, Xu H et al (2021) The distribution of posterior malleolus fracture lines. Foot Ankle Int 42(7):959–66. https://doi.org/10.1177/1071100721996700
16 Liu Y, Lu H, Xu H et al (2021) Characteristics and classification of medial malleolar fractures. Bone Joint J 103-b(5):931–8. https://doi.org/10.1302/0301-620x.103b5.Bjj-2020-1859.R2
17. Su Q, Zhang Y, Liao S et al (2019) 3D computed tomography mapping of thoracolumbar vertebrae fractures. Med Sci Monit 25:2802–2810. https://doi.org/10.12659/msm.915916
18. Ni M, Lv ML, Sun W et al (2021) Fracture mapping of complex intra-articular calcaneal fractures. Ann Transl Med 9(4):333. https://doi.org/10.21037/atm-20-7824
19. Guo X, Liang X, Jin J et al (2021) Evaluation of Sanders type 2 joint depression calcaneal fractures in 197 patients from a

single center using three-dimensional mapping. Med Sci Monit 27:e932748. https://doi.org/10.12659/msm.932748
20. Guo X, Liang X, Jin J et al (2021) Three-dimensional computed tomography mapping of 136 tongue-type calcaneal fractures from a single centre. Ann Transl Med 9(24):1787. https://doi.org/10.21037/atm-21-6168
21 Yu Q, Li Z, Li J et al (2022) Calcaneal fracture maps and their determinants. J Orthop Surg Res 17(1):39. https://doi.org/10.1186/s13018-022-02930-y
22 Athavale SA, Joshi SD, Joshi SS (2010) Internal architecture of calcaneus: correlations with mechanics and pathoanatomy of calcaneal fractures. Surg Radiol Anat 32(2):115–22. https://doi.org/10.1007/s00276-009-0563-2
23 Rammelt S, Swords MP (2021) Calcaneal fractures-which approach for which fracture? Orthop Clin North Am 52(4):433–50. https://doi.org/10.1016/j.ocl.2021.05.012